Exploiting Radio Irregularity in Wireless Networks for Automated People Counting

Wei-Chuan Lin, *Student, IEEE,* Winston K.G. Seah, *Senior Member, IEEE,* and Wei Li, *Member, IEEE,*

Abstract

The Internet of Things (IoT) refers to a large cyber-physical system centered around the Internet that connects not just computer systems but a plethora of systems, devices, and objects, collectively referred to as "Things". It encompasses technologies for identification and tracking, sensing and actuation, both wired and wireless communications, and also, intelligence and cognition. Wireless communications, which is an integral part of IoT, suffers from radio irregularity – a phenomenon referring to radio waves being selectively absorbed, reflected or scattered by objects in their paths, e.g., human bodies that comprises liquid, bone and flesh. Radio irregularity is often regarded as a problem in wireless communications but, with the envisioned pervasiveness of IoT, we aim to exploit radio irregularity as a means to detect people. We demonstrate how radio signal fluctuations arising from radio irregularity can be used to provide a low-cost alternative to dedicated sensing systems for indoor automated people counting.

Index Terms

Automated People Counting; Infering human activity; Internet of Things; Wireless Sensor Network;

- *Wei-Chuan Lin, and Winston K.G. Seah are with the School of Engineering and Computer Science, Victoria University of Wellington, P.O. Box 600, Wellington 6140, New Zealand. E-mail: {wei-chuan.lin, winston.seah}@ecs.vuw.ac.nz*
- *Wei Li is with the Department of Electrical and Computer Engineering, University of Victoria, P.O. Box 3055, Victoria, B.C. V8W 3P6, Canada. Email: wli@ECE.UVic.CA*

Exploiting Radio Irregularity in Wireless Networks for Automated People Counting

1 Introduction

The Internet has grown beyond connecting computer systems and platforms that run applications to meet endusers' computing and communication needs to connecting a plethora of systems, appliances, devices, objects, etc., collectively referred to as "Things", turning it into a large cyber-physical system and giving rise to a new paradigm known as the Internet of Things (IoT) [1]. Likewise, the technologies that the IoT encompasses extend beyond computation and communication, to identifcation and tracking, sensing and actuation, and even intelligence and cognition. Ensuring connectivity in the IoT is increasingly reliant on wireless communications as connected devices become more ubiquitous and embedded into our daily living space.

The key technology in wireless communications is radio frequency (RF) transmission. When an RF signal propagates within a medium, it may be reflected, diffracted, and scattered. Each effect occurs to a different extent in various media, depending on factors such as wavelength and intensity of the wave, thickness and physical composition (permittivity and permeability) of the medium. The human body comprises liquid, bone and flesh, which selectively absorb, reflect or scatter RF signals, leading to the phenomenon known as *radio irregularity*. Consequently, in the presence of human activity within a network, the radio irregularity phenomenon is seen as signal strength fluctuations at the receiver, and the degree of signal fluctuation exhibits a significant level of correlation to the level of human activity in the network. Researchers have exploited this phenomenon in intrusion detection [2] and device-free localization applications [3].

Applications like automated people counting cannot tolerate false positives that result in overcounting, giving inaccurate data that are used for forecasting and resource allocation. People counting is extensively used in different industries, including retail (stores, malls and shopping centres), colleges and universities, government facilities, government non-profits organizations, visitor centres, libraries, museums and art galleries. In the retail industry, it is a form of intelligence-gathering that helps a retailer determine the percentage of visitors who actually make purchases. This is a key performance indicator of a store's performance as compared to just looking at the sales data. It also helps the management to optimize the usage of staff resources, e.g. deploy more staff during peak periods and cutting down during lull periods in order to save wages. For building management purposes, people counting is used to ensure that the safe level of occupancy is maintained.

With the emergence of IoT leading to pervasive wireless communication devices, radio irregularity

which has often been viewed as a problem can instead be exploited for automated people counting with minimal additional hardware and installation costs. In the next section, we examine the related research on automated people counting with a focus on indoor use cases. We then present our approach to indoor automated people counting based on the signal fluctuations arising from radio irregularity. This is followed by the discussion of the experimental study and the application of discriminant analysis to process the results obtained from tests carried out indoors within a building before concluding the paper.

2 Related Work

The GreenSpace organization provides a guide to commercially available automated people counting technology [4] among which infrared beam counters, thermal counters and video/CCTV cameras are the commonly used indoor people counting technologies.

2.1 People Counting Methods

The simplest and possibly cheapest approach is a single-beam infrared (IR) counter placed across an entrance. However, such a counter suffers from numerous drawbacks and is only suitable detecting someone passing, e.g. entering/leaving a shop. These commonly used counters have very high percentage of errors when multiple persons cross their monitoring area at a time. When multiple (IR) beams are deployed with careful placements strategies and coupled with wireless communications for transferring the acquired data to a base station computer that uses artificial intelligence techniques for processing, a more accurate and versatile people counting system can be realized [5].

People counters that use thermal imaging are typically mounted overhead and have the ability to simultaneously maintain separate counts for multiple people moving in two directions (in and/or out). The IR images captured by the heat detectors are then processed to determine the number of people [6]. Video-based people counters work on video streams obtained through video/CCTV camera which are then run through intelligent video-processing techniques to identify and count the people in the video. The accuracy of such approaches can vary according to the level of ambient lighting and background colour contrasts [7]. Hybrid approaches combining IR and video cameras, together with neural networks, have been proposed to improve the accuracy of visual-based automated people counting [8].

2.2 Radio-based Detection and Counting Methods

It was first reported in [9] that the shadowing effect caused by an object moving between two communicating wireless devices can be used for detection purposes. In particular, a human body comprises liquid, bone and flesh, that selectively absorb, reflect or scatter RF signals, leading to the phenomenon known as *radio irregularity*. This phenomenon has been extensively used for device-free localization in wireless networks [3]. Radio Tomographic Imaging [10] measures the attenuation of signals across wireless links

between many pairs of nodes in a wireless network to create ”images” of objects moving within the network area. The variance of measured received signal strength (RSS) on the links in a network has also been used to infer the locations of people or objects moving in the network deployment area [11]. This approach utilizes a statistical model for the RSS variance as a function of a person's position with respect to the transmitter and receiver locations. The approach adopted by [9] has also been extended in [12] for outdoor people counting by measuring the RSS level measured at the receiver. The reliance on (absolute) RSS values, however, has a drawback during deployment, which is the need to take into consideration the channel model and other related factors like the impact of path loss and fading. These approaches also require complex signal processing techniques and a calibration phase for each deployment environment, and this can significantly affect the ease of deployment.

It has been observed in [2] that human movement through the path of the radio signal causes the histogram of the absolute RSS values to become more spread; this is manifested quantitatively as higher standard deviation. However, the standard deviation varies significantly across environments, making it difficult to define a universal threshold to detect movement in terms of these first order statistics. While also exploiting the RSS spread caused by human movement, the approach adopted in [2] focused on the fluctuation in signal strength instead, in order to reduce the impact of channel models and other environmental factors. However, there are false positives reported in their results which are deemed to be acceptable in the intrusion detection application considered in that work.

3 Detection using RSSI Fluctuations

3.1 RSSI fluctuations caused by human activity

Most, if not all, the approaches that use the variance of RSS caused by human motion across the signal transmission paths require complex signal processing techniques and a calibration phase for each deployment environment, and this can significantly affect the ease of deployment. In our scheme, we adopt a network-oriented approach that relies on RSS information of received packets which can be easily obtained from device drivers of wireless network interfaces when the packets are received. A key goal of our approach is to be able to easily utilize the existing wireless transmitters and receivers already deployed in the environment without the need for accurate channel models nor complex signal processing techniques. We extend the method of using Received Signal Strength Indicator (RSSI) fluctuations proposed in [2] which has shown that two consistent patterns of RSSI fluctuations can be observed for two key scenarios of interest to us, namely, without human movement and with human movement across the signal transmission path, as shown in Fig. 1. The histogram of RSSI readings shows narrower distribution when there is no human movement across the signal path, i.e., there is less fluctuation across RSSI readings (Fig. 1a). On the other hand, the wireless signals fluctuate in the presence of human movement resulting in the spread out distribution of RSSI fluctuation shown in Fig. 1b.

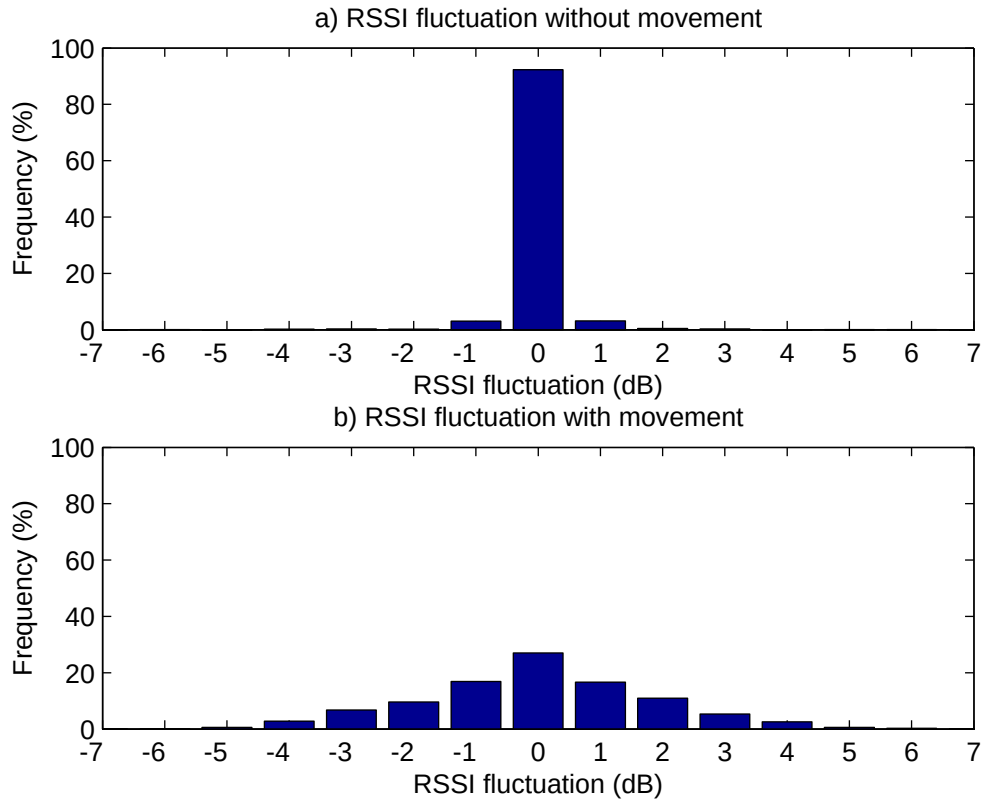

Fig. 1. RSSI Fluctuation Patterns [2]

3.2 Human Detection

Our proposed algorithms computes the fluctuation between the RSSI of packets received at a receiver. The absolute RSSI readings for packets recorded at the receiver over a period of time is shown in Fig. 2. From the absolute RSSI readings, the fluctuation of RSSI readings is calculated, as shown in Fig. 3.

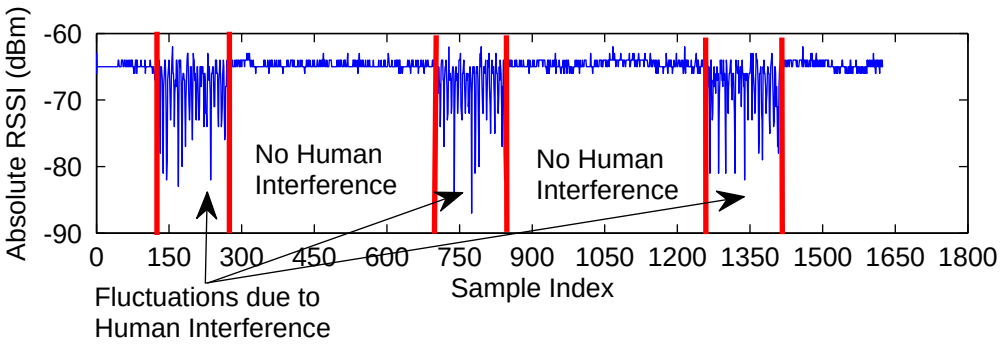

Fig. 2. Absolute RSSI reading

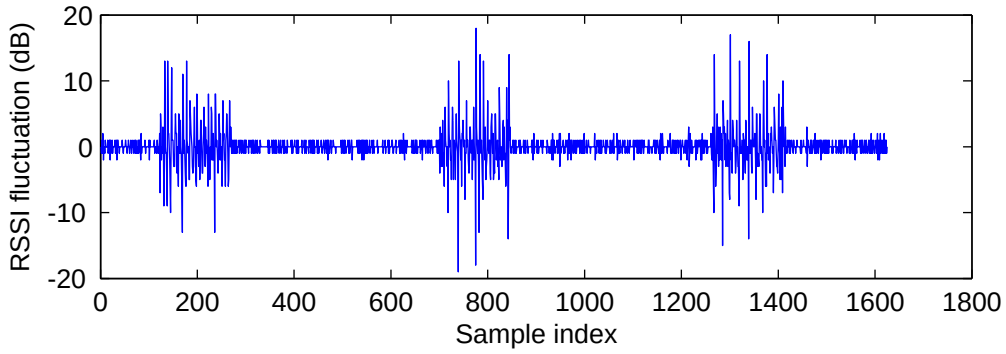

Fig. 3. RSSI Fluctuation

We then define a sliding window of n samples, where n is a parameter that can be tuned to achieve the desired accuracy for the target environment. In our example, a sliding window of size $n = 10$ is used to observe the behaviour of RSSI fluctuation. Therefore, a window of RSSI fluctuations at sample 200 is shown in Fig. 4.

At sample 200, using the window of 10 previous readings, the mean and standard deviation are computed as 0.2727 and 4.6280 respectively. We then map the RSSI fluctuations into the normal distribution with the mean and standard deviation for that window, i.e. $\mu = 0.2727$ and $\sigma = 4.6280$, as shown in Fig. 5a representing the case where the signal has been subjected to interference by human movement across its path. Similarly, the normal distribution of RSSI fluctuation at sample 600, where there is no movement, is shown for comparison in Fig. 5b. From the graphs, we compute the probability of the RSSI

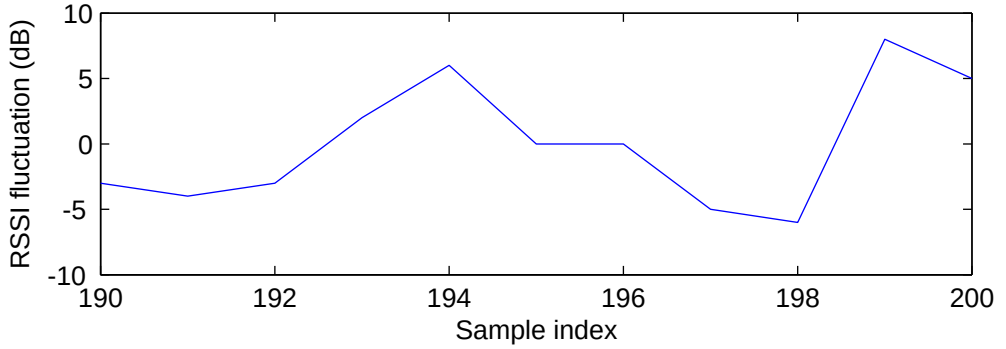

Fig. 4. RSSI fluctuations over a window size of 10

fluctuation falling within the range [-1,1] (i.e. area under the curve from -1 to 1) to be 0.17078 for the case where there is movement across the signal path (i.e. sample 200) and 0.84303 for the case where there is no movement (sample 600). For the dataset shown in Fig. 2, we compute the probability of falling with the fluctuate range [-1,1] and plot the results as shown in Fig. 6. As shown, the probability of fluctuations

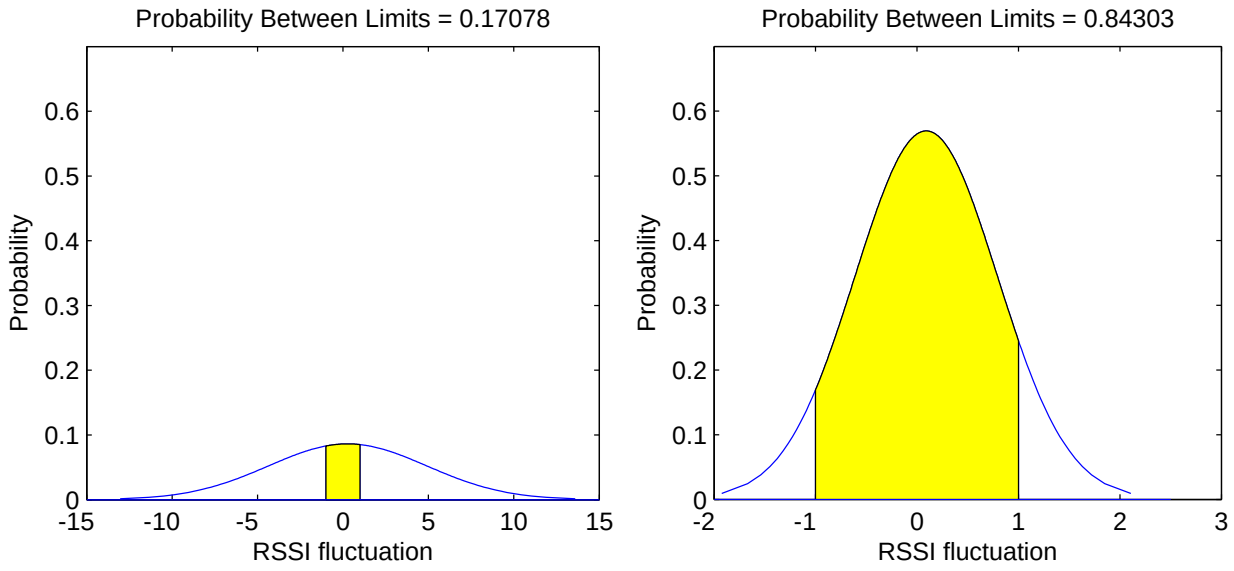

(a) Sample 200 (movement)

(b) Sample 600 (no movement)

Fig. 5. Normal distribution showing probability in fluctuation range [-1,1]

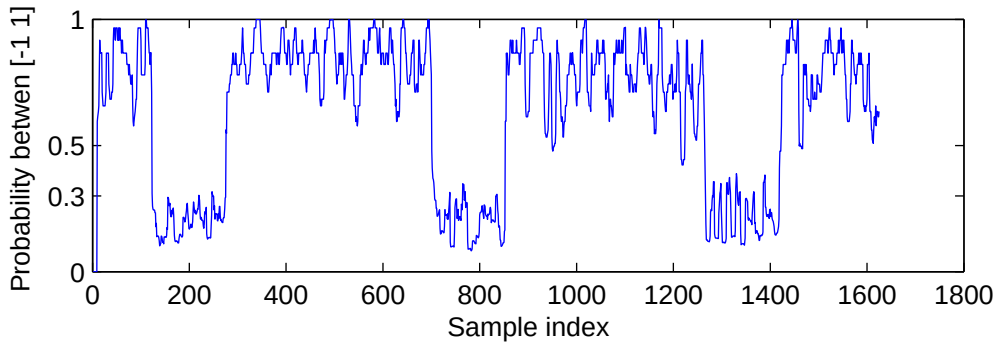

Fig. 6. Probability of fluctuation within [-1,1] for RSSI readings in Fig.2

falling in the range of [-1, 1] is below 0.3 in the presence of human movement. Hence, a probability value that is higher than 0.3 implies no human movement. Based on this threshold, we then infer from the results whether or not there has been human movement across the signal path, and the results are shown in Fig. 7.

The approach used in [2] has resulted in false positives as shown in Fig. 8a. We applied our approach to the dataset used by the detection algorithm [2] that produced the results shown in Fig. 8a, and confirmed that our algorithm is able to achieve better accuracy in eliminating false positives, as shown in Fig. 8b.

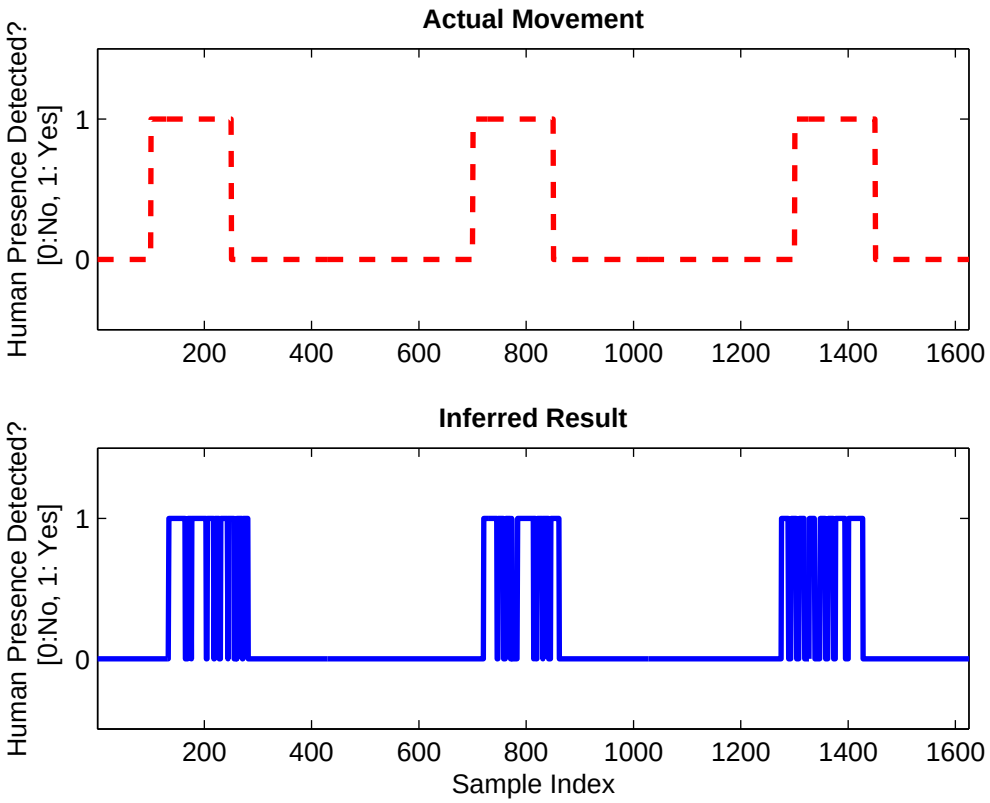

Fig. 7. Inferred presence of human movement using RSSI Fluctuations

4 Pedestrian Traffic Monitoring

Accurate detection of human movement is just the initial step to achieving the goal of automated people counting. The next step is the ability to infer that more than one person has crossed the area of interest.

4.1 Single transmitter-single receiver configuration

First, a series of experiments were conducted to observe the precision of the detection algorithm in a realistic indoor environment, namely, a corridor in a university building, as shown in Fig. 9, where the two red dots indicated by the arrows refer to the transmitter/receiver pair using IEEE802.15.4 technology. The devices are spaced 1.5m apart (width of corridor) and placed at a height of 1.1m, on a ledge. Each data collection duration was 300 seconds with inter-packet interval time of 0.15 seconds, during which the number of people who have walked past the devices were recorded and tagged with the time. Fig. 10 shows the results for one data collection period, during which nine persons walked through individually and two pairs of people past while walking close to each other, at the sample index of 484 and 925. In the detection results, shown in Fig. 10, a total of 11 movements were detected. It is clear that detecting two people walking side by side is a major challenge as the RSSI fluctuations arising from one and two persons passing are quite indistinguishable.

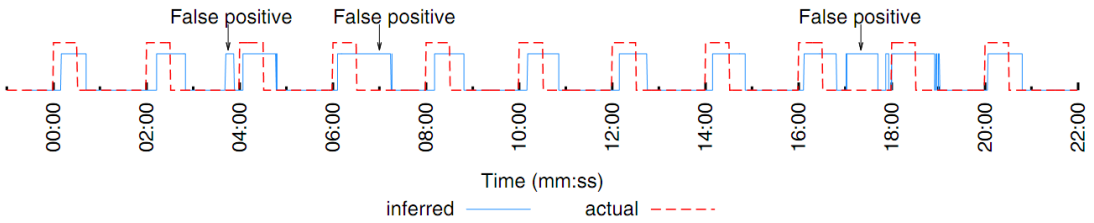

(a) False positives by detection method in [2]

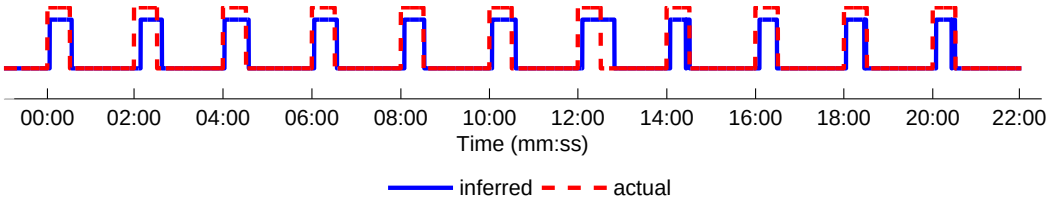

(b) Movement detected by our method

Fig. 8. Detection results using dataset of [2]

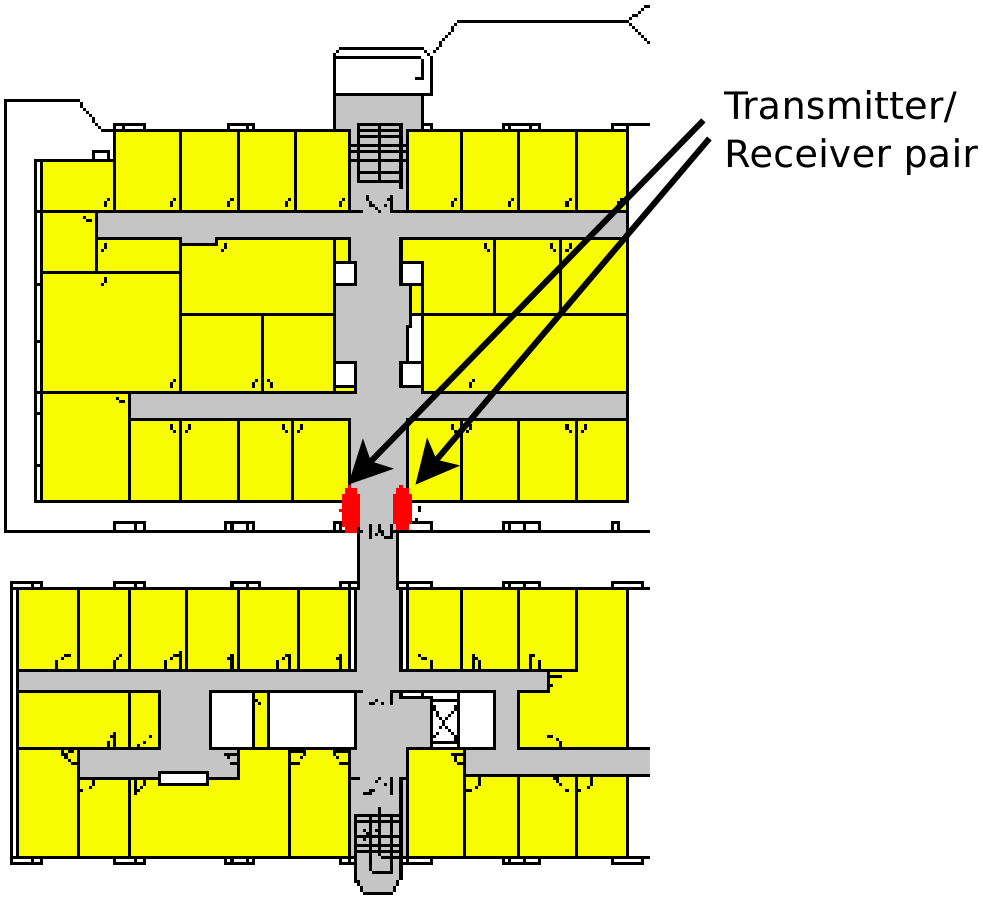

Fig. 9. Deployment along corridor of building in university

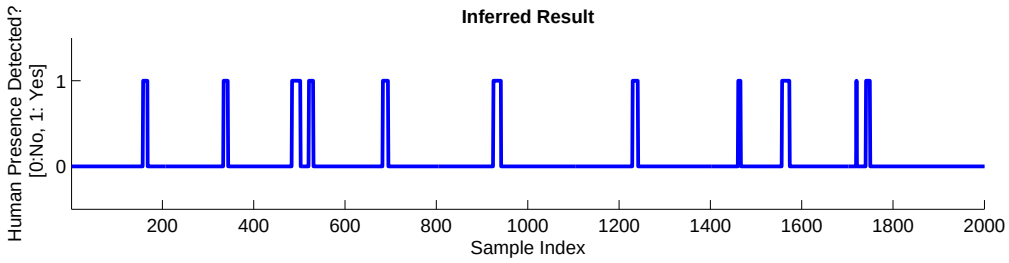

Fig. 10. Detection of pedestrian traffic along corridor

4.2 Single transmitter-multiple receiver configuration

In a pervasive network environment like IoT, it is not inconceivable to have numerous small wireless devices present. A conceptual deployment scenario like that shown in Fig. 11 can be assumed, and we look at a subset configuration of one-transmitter and two-receivers as shown in Fig. 12.

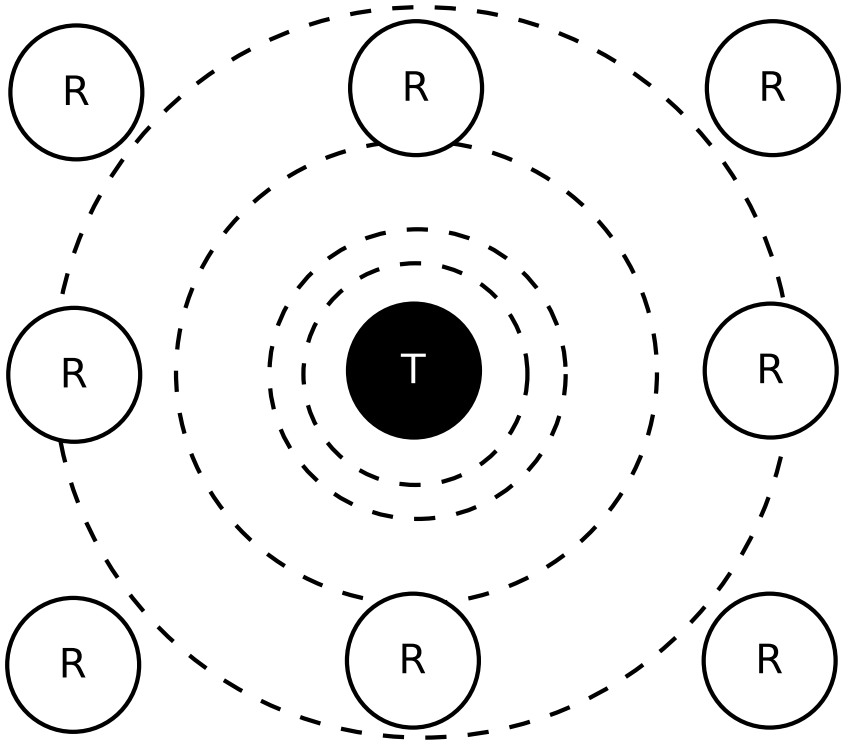

Fig. 11. Conceptual Configuration

Using the one-transmitter two-receiver configuration, the transmitter broadcasts packets at a rate of one packet every 0.15 seconds. Receiver R_1 is 1.5m from transmitter T (d_1 = 1.5m)and R_2 is 1.5m from R_1(d_2 = 1.5m). As two persons walk along the path between T and the two receivers in the direction shown in Fig. 12, they first cross the T-R_2 signal transmission path, followed by the T-R_1 signal path.

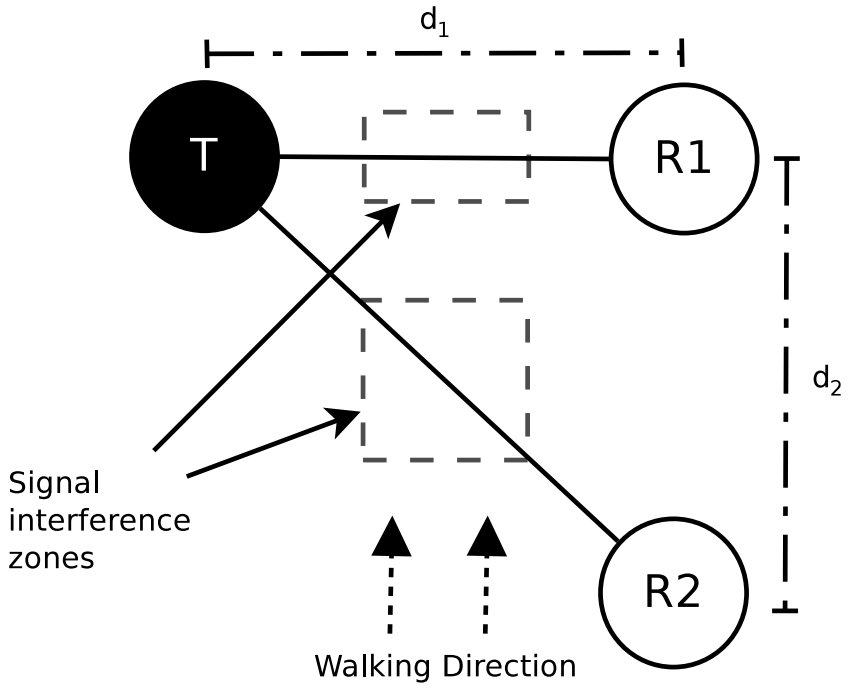

Fig. 12. One-Transmitter Two-Receiver Configuration

A key point to note is the different signal interference zones that result from the movement of the two persons.

First, we collected data for one person walking across the signal transmission path, passing first R_2 then R_1 to be used as the reference case. The detection results correctly show that one person passed at around the time of sample 100 and another at around sample 200, as shown in Fig. 13. Intuitively, the detection result at sample 100 is more logical since the person passed R_2 first, then R_1. However, as the two receivers at very close to each other, having the two receivers showing signal fluctuations at almost the same instant is also likely especially when the person is walking fast.

Next, we collected data for the case of two persons walking side-by-side in the direction of R_2 to R_1 as shown in Fig. 12. We expect that the detection duration of T-R_2 should be longer than T-R_1. This is because the T-R_2 signal experienced a longer duration of interference than the T-R_1 signal. The detection result of two people walking from R_2 to R_1 shown in Fig. 14 confirms our hypothesis. However, we also observed a false positive detection at sample 64. As the two receivers are placed closed to each other, 1.5m apart, we can assume that it is unlikely for a moving object to be detected by one receiver but not the other. Therefore, by comparing and matching the data from both receivers, we can perform a simple optimization process to remove such false positive detections, to achieve the desired results as shown in Fig. 15.

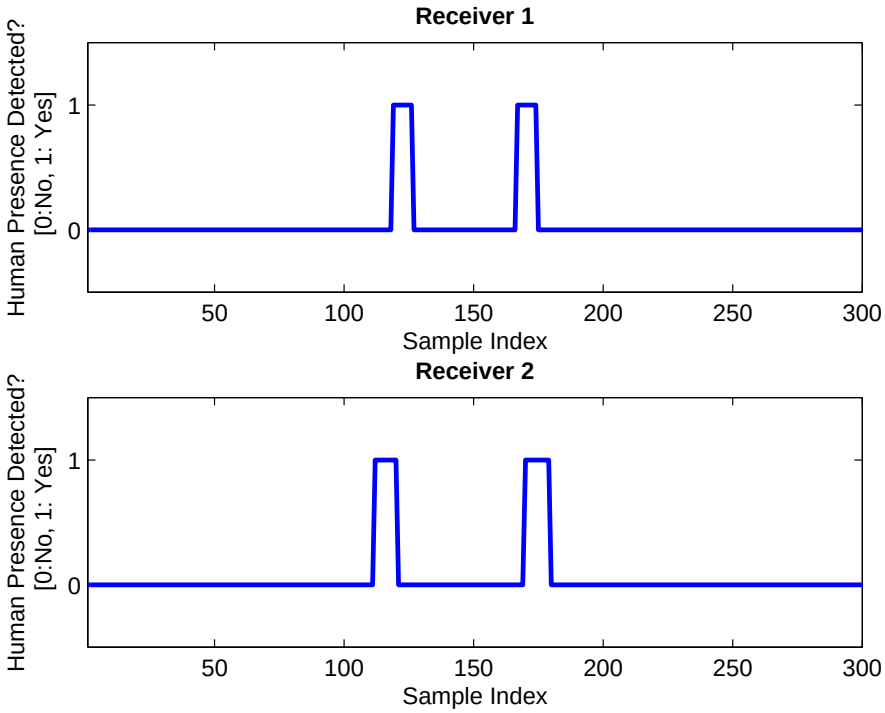

Fig. 13. One person walking in the direction of R2 to R1

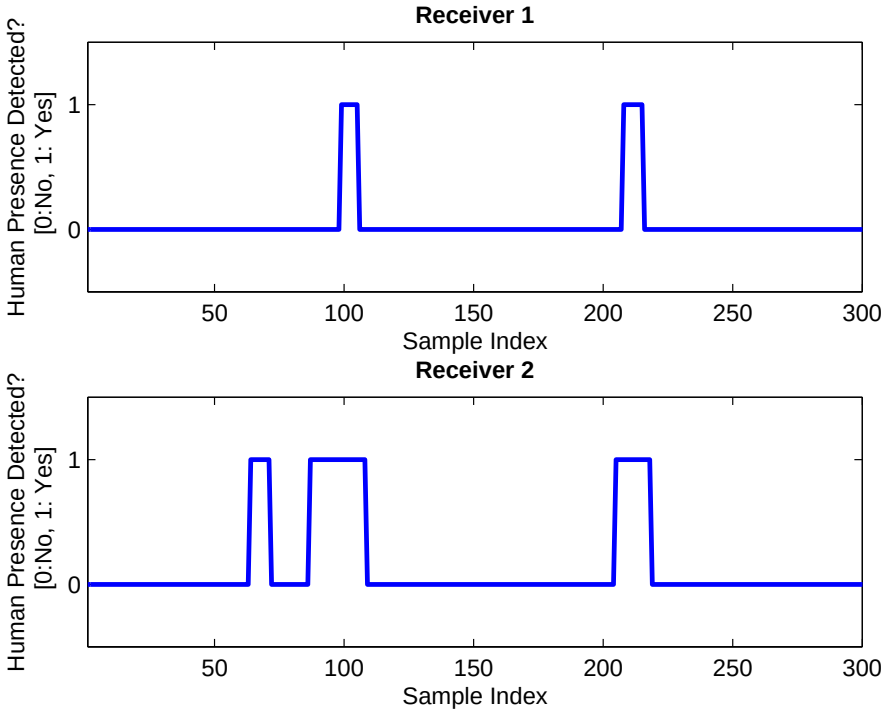

Fig. 14. Two people walking in the direction of R2 to R1

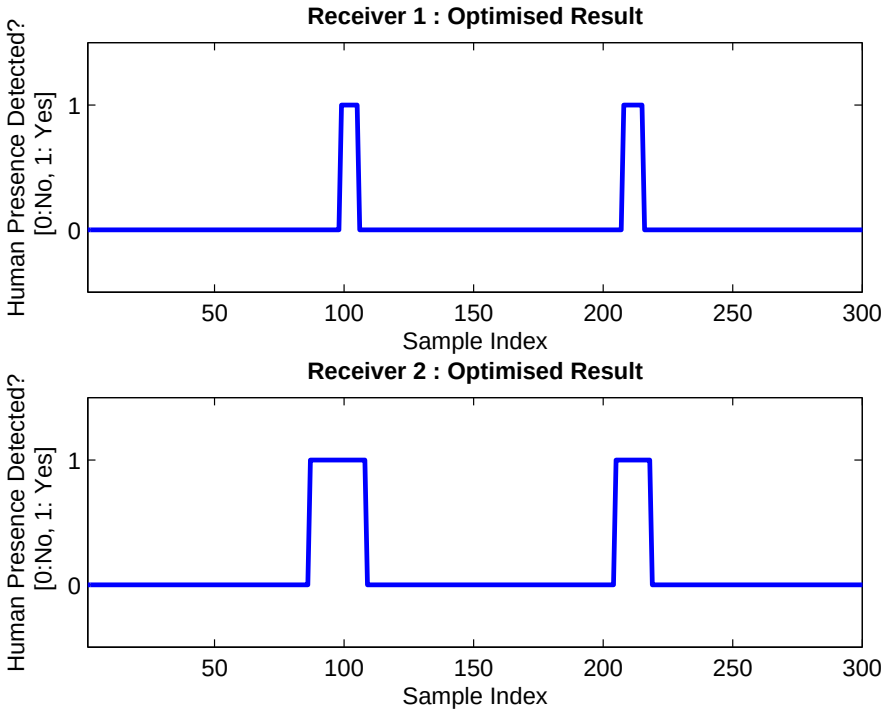

Fig. 15. Optimised Result of multiple receivers

5 Enhanced Accuracy for People Counting

5.1 Standard Deviation of RSSI fluctuation Approach

Although the use of the probability density function has eliminated the occurrence of false positives, a major limitation is that it disregards information from the distribution of RSSI fluctuations that lie outside the region between -1 and +1. This is undesirable as the distribution of RSSI fluctuations has been shown to be a good indication of the size or crowd density of moving objects [13].

In the standard deviation detection approach, we compute the standard deviation of samples within a sliding window. Signal interference due to human motion causes rapid RSSI fluctuations which results in an increased standard deviation. For example, at sample 200, the standard deviation is 4.6280 and at sample 600, the standard deviation is 0.6325. For the dataset shown in Fig. 2, we compute the standard deviation of RSSI fluctuation and the computed results are shown in Fig. 16, where the standard deviation of RSSI fluctuations being higher than 2 implies the presence of human movement. In addition, more information can be derived from the data, such as, the peak of standard deviation. We infer the existence of human movement based on the standard deviation threshold and the results are shown in Fig. 17.

5.2 Multiple Object Detection Setup

In order to exploit the effect of RSSI fluctuation caused by signal interference by a few people, we conducted a series of experiments with a variable group size (ranging from one to five people) under

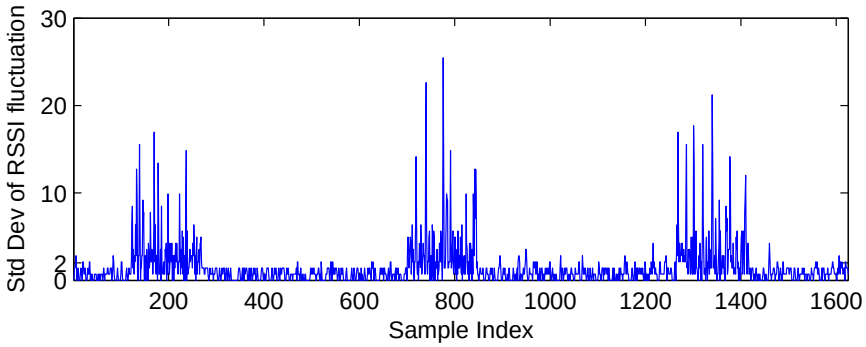

Fig. 16. Standard Deviation of fluctuation for RSSI readings in Fig.2

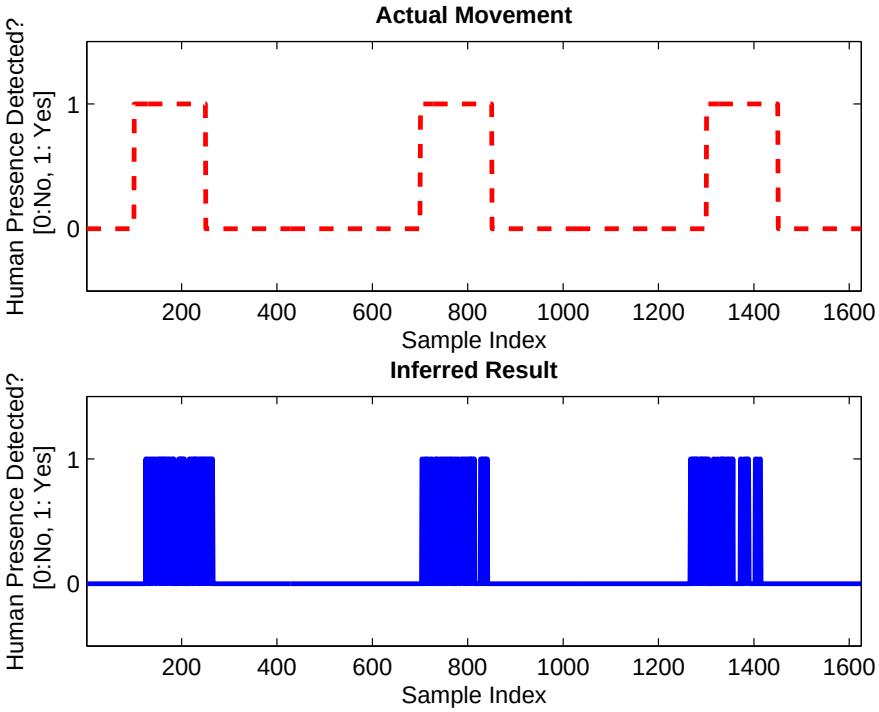

Fig. 17. Inferred presence of human movement using standard deviation approach

a controlled indoor environment. Sensor motes using IEEE802.15.4 wireless technology were deployed in a $6m \times 8m$ room in a one-transmitter two-receiver configuration (see Fig. 12.) The motes were placed at a height of 0.9m. Receiver R_1 was placed 3.5m from transmitter T (d_1 = 3.5m) and R_2 at 2m from R_1(d_2 = 2m). The transmitter, T, broadcasts packets continuously in time intervals of 0.1s. The absolute RSSI values were recorded upon packet reception at the receivers. Then, groups comprising one to five people made five consecutive round trips between the transmitter and two receivers. Five experiments were conducted for each group.

5.3 Discriminant Analysis

Discriminant analysis is a method to find the linear combination of measurements which characterize two or more groups [14]. We let a finite number g denote the distinct number of groups which in our case is five (i.e. 1–5 persons). We refer to the G_i as groups where $i = 1, \ldots, 5$. There are two phases of discriminant analysis which are training and classification. During the training phase, a total of $g - 1$ orthogonal discriminant functions are constructed such that the groups differ as much as possible on discriminant score D. The form of the linear discriminant function is:

$$D = v_1 X_1 + v_2 X_2 + ... + v_i X_i + c \tag{1}$$

where

$$D = \text{discriminant score}$$

$$v = \text{the discriminant coefficient}$$

$$X = \text{the value of independent variable}$$

$$c = \text{a constant}$$

$$i = \text{the number of independent variables}$$

Once the discriminant functions are constructed, the discriminant analysis enters the second phase which is classification. The Fisher linear discriminant analysis is used for data classification. The key idea of Fisher linear discriminant is to find the line of projection that separates different groups.

5.4 Apply discriminant analysis to standard deviation of RSSI fluctuation

We use the standard deviation of RSSI fluctuations of detected movement as the primary dataset. For instance, the standard deviation of RSSI fluctuations of one of the experiments for one person is shown in Fig. 18. We utilize the information from each positive detection, particularly mean, standard deviation (std), coefficient of variation (CV), detection duration and area under the curve, to be the independent variables (IVs) in order to achieve high discrimination between groups.

We use the SPSS [15] software to perform discriminant analysis. For a total of 50 samples of each group, the mean of each independent variable is plotted in Fig. 19. Duration and area under the curve are the two most significant independent variables. The detection duration of R_1 is stable throughout all groups while the detection duration of R_2 steadily increases as the number of people increase. This trend is as expected for more time is needed to pass the T-R_2 transmission path than T-R_1. The area under the curve follows the same trends as longer detection duration makes the area under the curve larger.

Next, these independent variables are taken to construct the discriminant functions that maximize the separation between each group. In Table 1, it provides very high F values and lower Wilks' Lambda

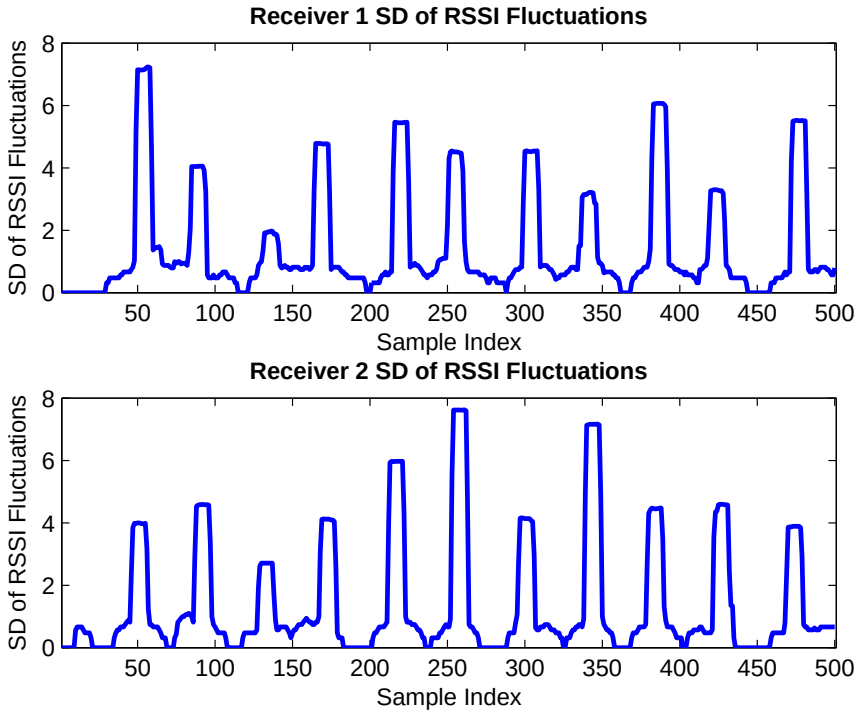

Fig. 18. Experimental Data for one person in a single experiment

IV	Wilks' Lambda	F	p-value
R_1 mean	0.773	17.986	0.001
R_2 mean	0.992	5.207	0.000
R_1 std	0.640	34.437	0.000
R_2 std	0.692	27.311	0.000
R_1 CV	0.485	65.034	0.000
R_2 CV	0.436	79.137	0.000
R_1 duration	0.633	35.572	0.000
R_2 duration	0.256	178.008	0.000
R_1 area	0.713	24.605	0.000
R_2 area	0.603	40.256	0.000

TABLE 1

Test of Equaltiy of Group Means

as evidence of significant difference in R_2 detection duration than any other independent variables. In addition, in statistical significance testing, the null hypothesis is rejected when the p-value is smaller than the significance level α which is 0.05. The results are considered to be statistically significant when null hypothesis is rejected.

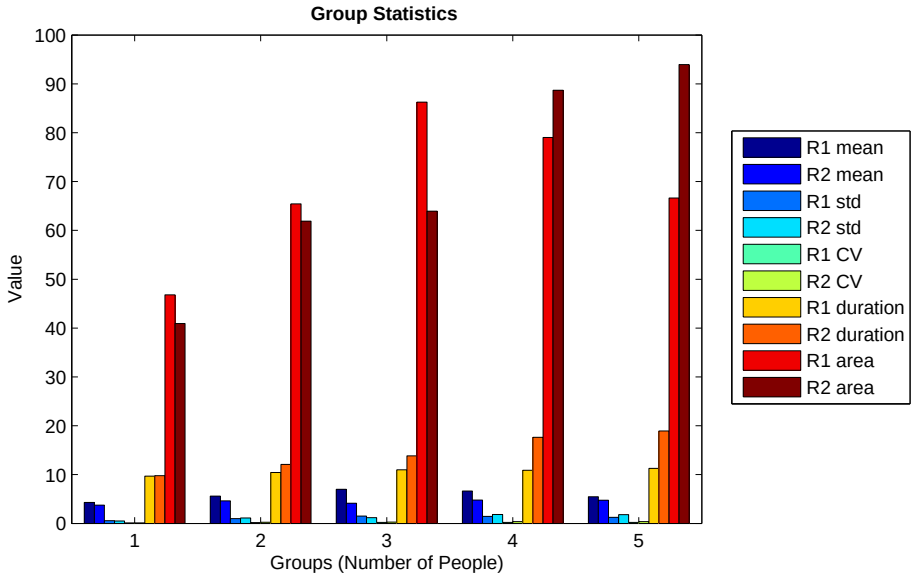

Fig. 19. Mean of independent variables of each group

Functions	Eigenvalue	% of variance	Canonical Correlation
1	5.717	82.9	0.923
2	0.952	13.8	0.698
3	0.146	2.1	0.357
4	0.084	1.2	0.279

TABLE 2

Table of Eigenvalues

The information of each discriminant function is shown in Table 2. There are five groups, namely 'one person' to 'five people' and as a result four discriminant functions are produced. With high Eigenvalue and percentage of variance, function 1 covers most total statistical population.

The relative importance of each independent variable in each discriminant function can be found by analyzing the structure matrix table. These 'Pearson' coefficients are discriminant loadings which act like factor loadings in factor analysis [16]. Generally, an absolute value of 0.3 is taken to be the threshold that separates a significant from an unsignificant variable. For example, we have five independent variables in discriminant function D_1, namely, 'R_1 CV', 'R_2 CV', 'R_1 duration', 'R_2 duration', and 'R_2 area' that discriminates between groups.

The discriminant function coefficient shows the contribution of each independent variable to the discriminant function. It operates like a regression equation. For example, the discriminant function D_1 and D_2 are shown below.

$$
\begin{aligned}
D_1 = &(0.26 \times R_1 mean) + (-0.837 \times R_2 mean) + \\
&(-1.033 \times R_1 std) + (0.999 \times R_2 std) + \\
&(17.142 \times R_1 CV) + (3.964 \times R_2 CV) + \\
&(0.298 \times R_1 duration) + (0.306 \times R_2 duration) + \\
&(0.011 \times R_1 area) + (0.002 \times R_2 area) - 10.805
\end{aligned} \tag{2}
$$

$$
\begin{aligned}
D_2 = &(0.863 \times R_1 mean) + (-1.044 \times R_2 mean) + \\
&(-1.023 \times R_1 std) + (1.046 \times R_2 std) + \\
&(17.026 \times R_1 CV) + (-6.788 \times R_2 CV) + \\
&(0.225 \times R_1 duration) + (-0.203 \times R_2 duration) + \\
&(0.017 \times R_1 area) + (-0.003 \times R_2 area) - 2.414
\end{aligned} \tag{3}
$$

	Function			
	1	2	3	4
R_1 mean	0.153	0.384	-0.047	0.477
R_2 mean	0.094	-0.088	0.243	0.464
R_1 std	0.275	0.361	-0.051	0.235
R_2 std	0.269	-0.109	0.049	0.486
R_1 CV	0.417	0.219	0.387	-0.162
R_2 CV	0.468	-0.093	0.070	0.603
R_1 duration	0.306	0.111	0.417	-0.296
R_2 duration	0.692	-0.411	-0.206	-0.098
R_1 area	0.191	0.438	0.020	0.372
R_2 area	0.326	-0.212	0.094	0.288

TABLE 3
Structure Matrix

Fig. 20 plots for all samples of discriminant functions 1 and 2 which cover 96.7% of variance. The group centroids are plotted from left to right as the number of people increase. This is a good indication that the groups are well discriminated by functions D_1 and D_2.

Finally, the classification is performed based on the discriminant score. The classification results are shown in Table 5. All perfect prediction cases lie on the diagonal. The classification results show 81.6% overall accuracy in detecting the number of people comprising a given group. Further, an overall accuracy of 97.9% was achieved in predicting individual head counts. For example, the actual head count of 250 samples is 750 and the predicted head count was 734.

	Function			
	1	2	3	4
R_1 mean	0.260	0.863	0.611	0.084
R_2 mean	-0.837	-1.044	0.843	0.460
R_1 std	-1.033	-1.023	-4.612	-0.471
R_2 std	0.999	1.046	-1.165	-0.934
R_1 CV	17.142	17.026	32.236	-12.682
R_2 CV	3.964	-6.788	2.522	12.729
R_1 duration	0.298	0.225	0.514	-0.358
R_2 duration	0.306	-0.203	-0.140	-0.146
R_1 area	0.011	0.017	-0.001	0.018
R_2 area	0.002	-0.003	0.005	0.012
(Constant)	-10.805	-2.414	-10.974	2.054

TABLE 4

Canonical Discriminant Function Coefficient

	NPeople	Predicted Group Membership					
		1	2	3	4	5	Total
Count	1	47	3	0	0	0	50
	2	3	46	1	0	0	50
	3	0	3	44	2	1	50
	4	0	3	7	31	9	50
	5	0	0	0	14	36	50
%	1	94	6	0	0	0	100
	2	6	92	2	0	0	100
	3	0	6	88	4	2	100
	4	0	12	14	62	18	100
	5	0	0	0	28	72	100

TABLE 5

Cassification Results

6 Conclusion

The use of radio irregularity resulting from the movement of human objects crossing the path of a radio signal to detect human presence has been demonstrated previously and applied to intrusion detection [2]. We have improved the accuracy by eliminating the occurrence of false positives but noted that the ability to detect more than one person remains a challenge if we rely on the characteristics of one signal's fluctuations. However, with pervasive networking brought about by the Internet of Things, the presence of numerous wireless communication devices allow us to study the fluctuations of multiple signals in

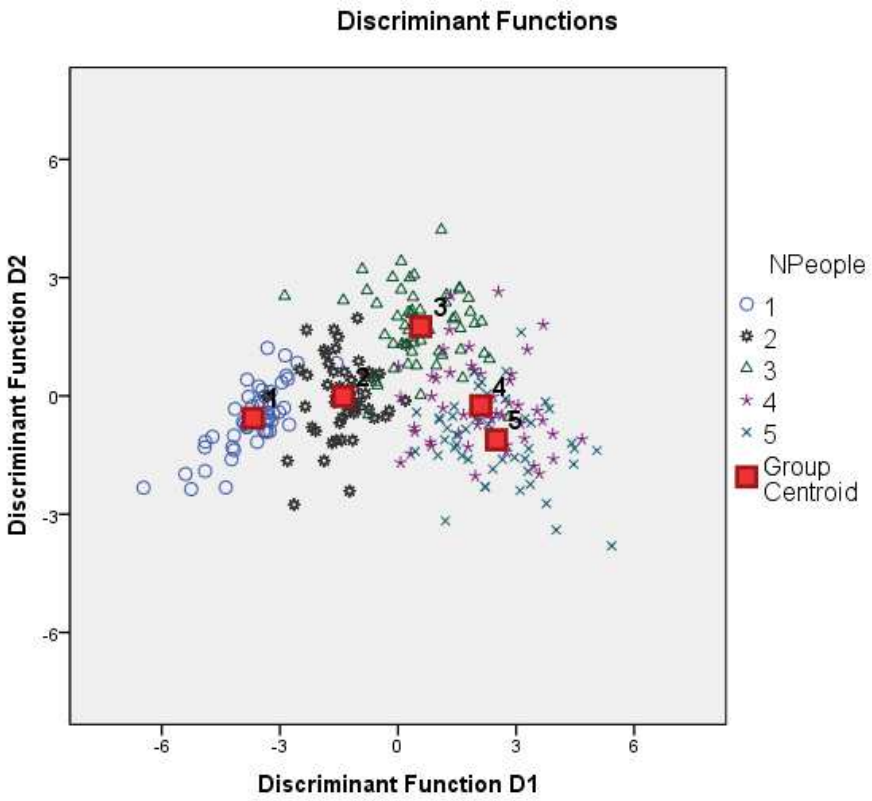

Fig. 20. Combined Group Plots of Discriminant Function 1 and 2

close proximity of one another as a result of human interference and deduce the number of human objects that have crossed the paths of these signals.

In this paper, we have proposed a network-oriented approach that utilizes RSS information of received packets to detect and count people when they cross the signal transmission paths. This information can be easily obtained from device drivers of wireless network interfaces when the packets are received and the goal of our approach is to be able to easily utilize the existing wireless transmitters and receivers already deployed in the environment. Our approach which is based on the RSSI fluctuations between consecutive packets does not require accurate channel models nor complex signal processing techniques.

Using a simple configuration of two receivers deployed in close proximity to each other, we have first demonstrated the ability to detect two persons walking side-by-side along a typical 1.5m wide corridor using a straightforward approach based on the difference in the periods of fluctuations experienced by the two signals paths as the two human subjects pass. We then extended our scheme to detect more human subjects using the same two-receiver configuration together with discriminant analysis to process the signal fluctuation data. We have been able to accurately detect and count up to five persons with an

accuracy of almost 98%.

From this study, we aim to show that the Internet of Things, which is a large cyber-physical system, can be exploited for applications like automated people counting without the need for specialized hardware. However, our method is not aimed to completely replace the specialized hardware for automated people counting but more as a complement to improve the accuracy. While the scheme in its current form requires further work to enhance its capabilities further, it presents an exciting opportunity to turn an existing indoor wireless communications network into a sensing system for automated people counting. As our ongoing and future work, we are extending the scheme for automated people counting in outdoor environments, e.g. to count visitors in public parks [4]. The scheme is also being adapted for use in the monitoring of wildlife in natural habitats.

ACKNOWLEDGMENTS

The authors would like to thank Dalice Sim, Statistical Consultant, for her invaluable assistance in the application of discriminant analysis to process our experimental data.

REFERENCES

[1] O. Vermesan *et al.*, *Internet of Things Strategic Research Roadmap*. European Commission - Information Society and Media DG, 15 September 2009.

[2] P. Lee, W. K. G. Seah, H. P. Tan, and Z. Yao, "Wireless sensing without sensors – an experimental approach," in *Proceedings of the 20th IEEE International Symposium on Personal, Indoor and Mobile Radio Communications (PIMRC)*, Tokyo, Japan, 13-16 September 2009.

[3] N. Patwari and J. Wilson, "RF Sensor Networks for Device-Free Localization: Measurements, Models, and Algorithms," *Proceedings of the IEEE*, vol. 98, no. 11, pp. 1961–1973, November 2010.

[4] GreenSpace, "A guide to automated methods for counting visitors to parks and green spaces." [Online]. Available: http://www.green-space.org.uk/downloads/greenSTAT/visitor_monitoring_guide.pdf

[5] E. Mathews and A. Poigne, "An echo state network based pedestrian counting system using wireless sensor networks," in *Proceedings of the International Workshop on Intelligent Solutions in Embedded Systems*, Regensburg, Germany, 10-11 July 2008, pp. 1–14.

[6] J. Nakamura, Y. Tomita, and S. Honda, "Algorithm for counting the number of persons using ir image processing," in *Proceedings of the IEEE Instrumentation and Measurement Technology Conference (IMTC)*, Hamamatsu, Japan, 10-12 May 1994, pp. 220–223.

[7] H. Celik, A. Hanjalic, and E. Hendriks, "Towards a robust solution to people counting," in *Proceedings of the IEEE International Conference on Image Processing (ICIP)*, Atlanta, GA, USA, 8-11 October 2006, pp. 2401–2404.

[8] I. Amin, A. Taylor, F. Junejo, A. Al-Habaibeh, and R. Parkin, "Automated people-counting by using low-resolution infrared and visual cameras," *Measurement*, vol. 41, no. 6, pp. 589 – 599, 2008. [Online]. Available: http://www.sciencedirect.com/science/article/B6V42-4R1MF05-1/2/214939e79cdc070f3e5fe6cca4b4000b

[9] K. Woyach, D. Puccinelli, and M. Haenggi, "Sensorless sensing in wireless networks: Implementation and measurements," in *Proceedings of the 2nd International Workshop on Wireless Network Measurement (WiNMee 2006)*, Boston, MA, USA, April 2006.

[10] J. Wilson and N. Patwari, "Radio tomographic imaging with wireless networks," *IEEE Transactions on Mobile Computing*, vol. 9, pp. 621–632, 2010.

[11] N. Patwari and J. Wilson, "Spatial models for human motion-induced signal strength variance on static links," *IEEE Transactions on Information Forensics and Security*, vol. 6, no. 3, pp. 791–802, September 2011.

[12] D. Puccinelli, A. Foerster, A. Puiatti, and S. Giordano, "Radio-based trail usage monitoring with low-end motes," in *Proceedings of the 7th IEEE International Workshop on Sensor Networks and Systems for Pervasive Computing (PerSeNS)*, Seattle, WA, USA, 21 March 2011.

[13] M. Nakatsuka, H. Iwatani, and J. Katto, "A study on passive crowd density estimation using wireless sensors," in *Proceedings of 4th International Conference on Mobile Computing and Ubiquitous Networking (ICMU)*, Tokyo, Japan, 11-13 June 2008.

[14] G. J. McLachlan, *Discriminant Analysis and Statistical Pattern Recognition.* John Wiley & Sons, Inc., 1993, vol. 35, no. 7.

[15] SPSS: An IBM Company, Homepage: http://www.ibm.com/software/analytics/spss/.

[16] R. B. Burns and R. A. Burns, *Business Research Methods and Statistics Using SPSS*. SAGE publication Ltd., 2008.